

# Sequence-Based OOK for Orthogonal Multiplexing of Wake-up Radio Signals and OFDM Waveforms

Alphan Şahin, *Member, IEEE*, and Rui Yang, *Member, IEEE*

**Abstract**—In this study, we propose an approach to construct on-off keying (OOK) symbols for wake-up radios (WURs) by using sequences in frequency domain. The proposed method enables orthogonal multiplexing of wake-up signals (WUSs) and orthogonal frequency division multiplexing (OFDM) waveforms. We optimize the sequences with a tractable algorithm relying on an alternating minimization by considering the reliability of WUSs in fading channels. We demonstrate the performance of four optimized sequences and compare with state-of-the-art approaches. We show that the proposed method improves the WUR performance by controlling the energy distribution in frequency domain while removing the interference-floor at OFDM receiver.

## I. INTRODUCTION

The functionality of the Internet has been expanded in many dimensions in recent years. The inclusion of the Internet of things (IoT) with a large number of connected devices in the communication networks significantly changes the role of the Internet in our daily life and, in many situations, the way we interact with the things around us and the way they interact among them. Combined with other advanced technologies, such as artificial intelligence and cloud-based communication networks, IoT enables broad applications such as smart cars, smart home, smart cities, and smart farms. The root building blocks of those smart things are large number of IoT devices, e.g., cameras, actuators, and any small and low-cost electronics which may be wired or connected wirelessly.

Building the networks with IoT devices faces many challenges. As most of the IoT devices are the electronics connected remotely and powered by batteries, minimizing the power consumption to maintain long battery life over multiple years is one of the key design criteria. Since many IoT devices only need to operate with very long duty cycle, e.g., once a day or several days for smart meters, or only need to operate when there is a demand triggered by other rarely happened events, e.g., severe weather condition, the concept of wake-up radio (WUR) has been introduced for wireless IoT devices. With WUR, an IoT device can be put to sleep when it is not used. The wake-up radio receiver (WURx) is a specially designed receiver with extremely low power consumption or without using a battery at all. Such a WURx will wake up the IoT device once a wake-up signal (WUS) is received.

The concept of WUR has been introduced in several standards in the wireless industry. For example, the working group

of IEEE 802.11 has started a project to create a specification amendment [7], named as 802.11ba, for Wi-Fi devices which may be used for IoT applications [8]. 3GPP has also started a discussion to include protocols that enable WUR functionalities. WUR should be a simple and low-cost radio without complex signal processing components (e.g., discrete Fourier transform (DFT)) and the corresponding WUS may not need to be very sophisticated in some cases. However, the design and generation of such a signal are not straightforward when considering the efficiency of the overall network and the usage of WUSs in future IoT applications. For example, using a dedicated resource (frequency or time) for transmitting WUS is inefficient, and combining it with other signals (e.g., orthogonal frequency division multiplexing (OFDM) signal) without interfering with each other is highly desirable. In this paper, we will explore the ideas of multiplexing of WUS with on-off keying (OOK) symbols and OFDM signals for data communication with other devices.

In the literature, several modulation schemes are proposed for WURs. For example, in [1], a special bit stream which generates a WUS with OFDM symbols are proposed by considering IEEE 802.11a/g/n packet structure. One of the proposed bit streams is constructed such that it purposely yields OFDM symbols with high peak-to-average-power ratio (PAPR) and the location of the peak sample is controlled in time to achieve pulse-position modulation (PPM). Although the method has its own merit, in practice, OFDM symbols with high PAPR may not be reliable. The power back-off due to the high peak sample may limit the coverage range. The distortion due to non-linear hardware can also cause spectral growth which can violate the adjacent-channel interference (ACI) requirements of some standards. Another strategy mentioned in [1] is to map the low-power constellation points to the lower half of the channel bandwidth, and high-power points to the upper half to encode a bit 0 (and vice versa for bit 1), i.e., frequency-shift keying (FSK) which is also exploited in several WURx designs, e.g., [2]. In [3] and [4], a scheme which modulates the frame length by using multiple consecutive Wi-Fi or Bluetooth Low Energy (BLE) packets is introduced for WURs. The main bottleneck with frame-length modulation is that the data rate can be very low as the WUS requires many consecutive packets. In addition, the bit error rate (BER) performance can degrade drastically as the continuity of the packets for WUR can be broken if another station accesses the wireless medium. In [5], OOK symbols in a WUS are generated through by modulating OFDM symbols via high-power and low-power constellation points for ON and OFF symbols, respectively, for low-data rates. Several other

Dr. Alphan Şahin and Dr. Rui Yang are affiliated with Inter-Digital, Huntington Quadrangle, Melville, NY. email: {alphan.sahin, rui.yang}@interdigital.com

modulation techniques for WURs can also be found in [6] and the references therein. To the best of our knowledge, the design of multiple OOK symbols within one OFDM symbol duration and the orthogonal multiplexing of WUS and OFDM waveforms have not been addressed yet.

For IEEE 802.11ba, it has been agreed that the WUS will be transmitted by using OOK symbols. The OFDM waveform parameters adopted in IEEE 802.11n/ac are considered as the baseline for the OOK symbol to reuse the existing 802.11n/ac transmitters. The bandwidth of WUS is decided to be 4 MHz and the OOK symbol duration is set to 2  $\mu$ s for high-data rate WUS, which is half of the IEEE 802.11n/ac OFDM symbol duration. To enable non-coherent detection, the bits for the wake-up payload are encoded with Manchester coding, which implicitly yields PPM. Several ways of generating the OOK symbols are proposed. For example, using the half of the 802.11n/ac OFDM symbols with 13 non-zero subcarriers (i.e., masked-based approach) or using a smaller inverse discrete Fourier transform (IDFT) with 7 non-zero subcarriers are some of the proposed methods to generate the OOK symbols (e.g., see [9] and the references in [10]). Multiplexing quadrature amplitude modulation (QAM) and OOK symbols in an orthogonal frequency division multiple accessing (OFDMA) framework (such as IEEE 802.11ax) has not been addressed in IEEE 802.11ba. One of the reasons is because the orthogonality OFDM and OOK symbols with the state-of-the-art designs cannot be maintained when their symbol durations are different.

In this study, we propose to construct OOK symbols within one OFDM symbol for WURs by using a fixed number of subcarriers. The proposed approach enables a radio to transmit WUSs without any interference to the other subcarriers which may potentially be utilized for the data transmission for the other users in the network. We particularly focus on OOK symbols with Manchester coding within an OFDM symbol for non-coherent detection. To increase the reliability of WUS, we optimize the sequences with a tractable algorithm by taking the leakage on the OFF period and the flatness of the corresponding waveform in time and frequency domain into account. The proposed algorithm is based on an algorithm called cyclic algorithm-new (CAN) which was proposed to generate a unimodular sequence with low integrated side lobe (ISL) metric [11]. A sequence generated with CAN can lead to significantly low PAPR when it is used in OFDM due to the low ISL of the sequence [12]–[14]. Hence, the ideal shape that CAN targets is a flat signal in time in terms of sample power. We extend CAN to generate any shape in time and utilize the derived algorithm, i.e., shaping with CAN (SCAN), to achieve orthogonal OOK symbols.

The rest of the paper is organized as follows. In Section II, we provide system models for the transmitter, channel, and receiver. In Section III, we discuss the sequences-based OOK and provide the details of the proposed algorithm, i.e., SCAN. In Section IV, we present numerical results based on IEEE 802.11n/ac waveform parameters. We conclude the paper in Section V with final remarks.

*Notation:* Hermitian operation is denoted by  $(\cdot)^H$ . The operations  $(\cdot)$  and  $(\cdot)^*$  reverses the order of the elements and

applies element-wise complex conjugation to their arguments, respectively. The operator  $\{\cdot\}_k$  gives the  $(k+1)$ th element of its argument. The 2-norm and infinity norm are denoted by  $\|\cdot\|_2$  and  $\|\cdot\|_\infty$ , respectively.  $\mathbb{E}\{\cdot\}$  represents the expectation operator. The field of complex numbers is represented by  $\mathbb{C}$ .  $\Re\{\cdot\}$  and  $\Im\{\cdot\}$  return the real part and the imaginary part of their arguments, respectively.

## II. SYSTEM MODEL

In this section, we provide the models for the wake-up radio transmitter (WUTx), multipath channel, and WURx.

### A. Wake-up Radio Transmitter

Consider a communication system where the transmitter generates a WUS by mapping the bits to the basis functions in a basis  $\mathcal{W}$ . In this study, we assume that  $\mathcal{W}$  consists of two basis functions, i.e.,  $\mathcal{W} = \{f_{s_i}(t) | i \in \{0, 1\}, \mathbb{E}\{|f_{s_i}(t)|^2\} = 1, 0 \leq t < T_s\}$ , and  $f_{s_0}(t)$  and  $f_{s_1}(t)$  correspond to the transmitted signals for  $b_m = 0$  and  $b_m = 1$ , respectively, where  $b_m$  is the  $m$ th bit in the WUS. The signal  $f_{s_i}(t)$  is constructed by mapping a sequence  $s_i \in \mathbb{C}^{L \times 1}$  from frequency domain using  $L$  contiguous orthogonal subcarriers to time domain as

$$f_{s_i}(t) = \frac{1}{\sqrt{P}} \sum_{k=0}^{L-1} \{s_i\}_k e^{j2\pi(k - \frac{L+1}{2})\Delta f t}, \quad (1)$$

where  $k$  is the subcarrier index,  $\Delta f$  is the subcarrier spacing,  $\|s_i\|^2 = P$ , and  $T_s = 1/\Delta f$ . Without loss of generality, we assume that  $L$  is an odd positive integer number, the element of  $s_i$  that corresponds to the DC tone is set to zero (i.e.,  $\{s_i\}_{\frac{L-1}{2}} = 0$ ), and  $P = L - 1$ . The center tone is not utilized because a DC blocker may be employed at the WUR. Assuming a cyclic prefix (CP) is used for the OFDM signal, to achieve orthogonal multiplexing of WUS and OFDM waveforms, a CP with the duration of  $T_{CP}$  is prepended to  $f_{s_i}(t)$ .

To enable non-coherent detection at the WUR, we assume that  $f_{s_i}(t)$  confines the symbol energy on the period denoted by  $\mathbb{M}_{\text{high},i} = (iT_{\text{active}}, (i+1)T_{\text{active}})$ , where  $T_{\text{active}} \leq T_s/2$  is the active duration for ON and OFF periods. This choice implicitly corresponds to PPM or a waveform generated via plain OOK waveform when bits are encoded with Manchester coding. For example, Manchester coding can result in  $\{0, 1\}$  and  $\{1, 0\}$  for  $b_m = 0$  and  $b_m = 1$ , respectively, and the plain OOK symbol duration is set to  $T_{\text{active}}$  for each coded bit.

We represent the ideal shape for  $|f_{s_i}(t)|^2$  as  $\Lambda_i(t)$  where  $\Lambda_i(t) = T_s/T_{\text{active}}$  for  $t \in \mathbb{M}_{\text{high},i}$  and 0 for  $t \in \mathbb{M}_{\text{low},i}$ , where  $\mathbb{M}_{\text{low},i}$  consists of the periods which contain low-energy samples. We assume that  $\mathbb{M}_{\text{high},i} \cap \mathbb{M}_{\text{low},i} = \emptyset$ ,  $\mathbb{M}_{\text{high},i} \cup \mathbb{M}_{\text{low},i} = [0, T_s)$ , and  $\mathbb{E}\{\Lambda_i(t)\} = 1$ .

### B. Channel Model

The wireless channel is modeled as an exponential power delay profile (PDP) with  $\mathcal{L}$  independent taps where the unnormalized power of the  $l$ th tap is expressed as  $e^{-\tau l}$  and  $\tau$  corresponds to the decay rate. Note that  $\tau = 0$  yields a uniform PDP. We assume Rayleigh distribution for the amplitude of each tap.

### C. Wake-up Radio Receiver

We assume that WUR skips the samples during CP durations and detects  $b_m$  by comparing the energy on active durations without any channel estimation. We also consider that WUR employs a second order Butterworth low-pass filter (LPF) where its cut-off frequency is denoted by  $f_c$ .

### III. SEQUENCE-BASED ON-OFF KEYING

In this section, we discuss sequence-based OOK and the corresponding algorithm, i.e., SCAN, to obtain the sequences.

#### A. Problem Formulation

In this study, our main goal is to find the sequence  $\mathbf{s}_i$  such that the Euclidean distance between  $|f_{\mathbf{s}_i}(t)|^2$  and  $\Lambda_i(t)$  is minimum while satisfying certain constraints related to the leakage during the OFF period and flatness in time and frequency.

In the sequel, we only consider the optimization of  $\mathbf{s}_0$  and omit the index  $i$  unless otherwise stated since  $f_{\mathbf{s}_0}(t)$  can be generated through  $f_{\mathbf{s}_1}(t)$ . For example, if  $T_{\text{active}}$  is chosen as  $T_s/2$ ,  $|f_{\mathbf{s}_0}(t)|$  can be the time-reversal of  $|f_{\mathbf{s}_1}(t)|$ . One way of achieving the time-reversal relationship between the basis functions is to relate  $\mathbf{s}_1$  and  $\mathbf{s}_0$  as  $\mathbf{s}_1 = \tilde{\mathbf{s}}_0$  or  $\mathbf{s}_1 = \mathbf{s}_0^*$  since the inverse Fourier transformation of  $\tilde{\mathbf{s}}_0$  and  $\mathbf{s}_1 = \mathbf{s}_0^*$  are  $f_{\mathbf{s}_0}(-t)$  and  $f_{\mathbf{s}_0}^*(-t)$ , respectively. The choice of  $\mathbf{s}_1 = \tilde{\mathbf{s}}_0$  reduces the hardware complexity at the transmitter since the transmitter can generate the basis functions by changing the order of the elements of  $\mathbf{s}_0$ . In the cases where  $T_{\text{active}}$  is less than  $T_s/2$ ,  $\{\mathbf{s}_1\}_k$  can be set to  $e^{-j2\pi k T_{\text{active}}/T_s} \{\mathbf{s}_0\}_k$  by exploiting the time-shifting property of the inverse Fourier transformation.

We express the distance between  $|f_{\mathbf{s}}(t)|^2$  and  $\Lambda(t)$  with root-mean-squared error (RMSE) as

$$\epsilon = \mathbb{E} \left\{ \left| |f_{\mathbf{s}}(t)|^2 - P\Lambda(t) \right|^2 \right\}^{\frac{1}{2}}. \quad (2)$$

The optimization problem that gives the optimal sequence for  $f_{\mathbf{s}}(t)$  can then be written as

$$\hat{\mathbf{s}} = \arg \min_{\mathbf{s}} \mathbb{E} \left\{ \left| |f_{\mathbf{s}}(t)|^2 - P\Lambda(t) \right|^2 \right\}^{\frac{1}{2}} + \lambda \|\mathbf{s}\|_{\infty} \quad (3)$$

$$\begin{aligned} \text{s.t. } c_1: \{\mathbf{s}\}_{\frac{L-1}{2}} &= 0 \\ c_2: |f_{\mathbf{s}}(0)|^2 &\leq P_{\text{first}} \\ c_3: |f_{\mathbf{s}}(t)|^2 &\leq P_{\text{leak}}, t \in \mathbb{M}_{\text{low}}, \end{aligned}$$

where  $P_{\text{first}}$  and  $P_{\text{leak}}$  are the desired values for the basis functions. In (3), we omit the frequency-shift component in (1) as it does not change the cost given in (2). We also regularize the elements of  $\hat{\mathbf{s}}$  by introducing a regularization term  $\|\mathbf{s}\|_{\infty}$  to the RMSE with a parameter denoted by  $\lambda \geq 0$ . When  $\lambda > 0$ , the regularization term in (3) applies a penalty if the sequence energy is localized on few elements and increase the reliability of the waveform against frequency-selective channels. The constraints  $c_1$ ,  $c_2$ , and  $c_3$  aim at zero DC tone, smooth ramp-up for the ON period, and low instantaneous power on the OFF period, respectively. Unfortunately, the argument of the expectation operator in (3) is a quartic function. Therefore, (3) is not a convex optimization problem. In the following part, we propose a tractable algorithm to solve (3).

#### B. SCAN: Shaping with CAN

To calculate the expected value in (3), we sample (2) within the period of  $[0, T_s)$ , where the  $p$ th sampling time is given by  $p/N \times T_s$ ,  $p \in \{0, 1, \dots, N-1\}$ , and  $N$  is the number of samples. The RMSE in (2) can then be calculated approximately as

$$\epsilon_s = \left( \frac{1}{N} \sum_{p=0}^{N-1} \left| \sum_{k=0}^{L-1} \{\mathbf{s}\}_k e^{j2\pi k \frac{p}{N}} \right|^2 - P\Lambda\left(\frac{pT_s}{N}\right) \right)^{\frac{1}{2}}. \quad (4)$$

Due to the convolution theorem, the maximum support of the IDFT of the  $|f_{\mathbf{s}}(pT_s/N)|^2$  is  $2L-1$  when  $N \geq 2L-1$ . Hence,  $N \geq 2L-1$  in 4 must also hold true to oversample the basis function  $|f_{\mathbf{s}}(t)|^2$ .

To enable tractable algorithms, we propose to modify (4) as

$$\begin{aligned} \epsilon_m &= \left( \frac{1}{N} \sum_{p=0}^{N-1} \left| \sum_{k=0}^{L-1} \{\mathbf{s}\}_k e^{j2\pi k \frac{p}{N}} - \sqrt{P}\{\mathbf{a}\}_p \{\boldsymbol{\theta}\}_p \right|^2 \right)^{\frac{1}{2}} \\ &= \frac{1}{\sqrt{N}} \|\mathbf{F}^H \mathbf{M} \mathbf{s} - \sqrt{P} \mathbf{A} \boldsymbol{\theta}\|_2, \end{aligned} \quad (5)$$

where  $\{\mathbf{a}\}_p = \sqrt{\Lambda(pT_s/N)}$ ,  $\mathbf{F} \in \mathbb{C}^{N \times N}$  is the DFT matrix,  $\mathbf{M} \in \mathbb{R}^{N \times L}$  is the mapping matrix,  $\mathbf{A} \in \mathbb{R}^{N \times N_{\text{active}}}$  is a semi-orthogonal matrix and obtained removing the zero columns of  $\text{diag}\{\mathbf{a}\}$ ,  $N_{\text{active}}$  is the number of non-zero elements in vector  $\mathbf{a}$ , and  $\boldsymbol{\theta} \in \mathbb{C}^{N_{\text{active}} \times 1}$  is a phase vector.

Both (4) and (5) are metrics to measure the distance between  $|f_{\mathbf{s}}(t)|^2$  and  $\Lambda(t)$ , i.e., if  $\epsilon_m$  is small,  $\epsilon_s$  also becomes small. However, (5) achieves it with a quadratic function, i.e., reduces the order of (4). The function in (5) can be thought as a generalization of the approach proposed in [11]. The main objective in [11] is to minimize the ISL metric of a unimodular sequence  $\mathbf{s}$ , i.e., equivalent to (4) for  $\Lambda(t) = 1$ ,  $|\{\mathbf{s}\}_k| = 1$ , and  $P = L$ . An iterative algorithm based on fast Fourier transform (FFT), called CAN, is derived by replacing the cost function in (4) with an another cost function, i.e., equivalent to a special case of (5). The discussion related to the validity of the modification is provided in [13]. Since the CAN minimizes the ISL metric of the sequence, it also targets the sequences that lead to low PAPR when the same sequence is used in frequency with an OFDM waveform, i.e., ultraflat polynomials [15], [16]. In this study, the proposed algorithm is based on CAN, called SCAN, and aim at the optimal sequences that lead to *any* ideal signal shape in time.

We first rewrite the optimization problem given in (3) by using the cost function given in (5) as

$$\hat{\mathbf{s}} = \arg \min_{\mathbf{s}, \boldsymbol{\theta}} \frac{1}{\sqrt{N}} \|\mathbf{F}^H \mathbf{M} \mathbf{s} - \sqrt{P} \mathbf{A} \boldsymbol{\theta}\|_2 + \lambda \|\mathbf{s}\|_{\infty} \quad (6)$$

$$\begin{aligned} \text{s.t. } c_1: \{\mathbf{s}\}_{\frac{L-1}{2}} &= 0 \\ c_2: |\{\mathbf{F}^H \mathbf{M} \mathbf{s}\}_0|^2 &\leq P_{\text{first}} \\ c_3: |\{\mathbf{F}^H \mathbf{M} \mathbf{s}\}_p|^2 &\leq P_{\text{leak}}, p \in \mathbb{N}_{\text{low}} \\ c_4: |\{\boldsymbol{\theta}\}_p|^2 &= 1, p \in \mathbb{N}_{\text{high}}, \end{aligned}$$

where  $\lambda$  is a Lagrange variable,  $\mathbb{N}_{\text{high}} = \{p | \{\mathbf{a}\}_p \neq 0\}$  and  $\mathbb{N}_{\text{low}} = \{p | \{\mathbf{a}\}_p = 0\}$ . The problem in (6) is still non-convex

due to the constraint  $c_4$ . However, the local optima can still be obtained by splitting (6) into two subproblems and solving them iteratively, i.e., alternating minimization.

For the  $i$ th iteration, the first subproblem for a given  $\mathbf{s}^{(i-1)}$  is given by

$$\begin{aligned} \boldsymbol{\theta}^{(i)} = \arg \min_{\boldsymbol{\theta}} & \|\mathbf{F}^H \mathbf{M} \mathbf{s}^{(i-1)} - \sqrt{P} \mathbf{A} \boldsymbol{\theta}\|_2 \\ \text{s.t.} & \quad |\{\boldsymbol{\theta}\}_p|^2 = 1, p \in \mathbb{N}_{\text{high}}. \end{aligned} \quad (7)$$

Although (7) is not a convex problem due to the unimodular vector constraint, the global optimum can be obtained via a closed-form solution given by  $\{\boldsymbol{\theta}\}_p = \angle\{\mathbf{F} \mathbf{M} \mathbf{s}\}_p$ . This is due to the fact that the support of the columns of  $\mathbf{A}$  do not intersect (i.e., semi-orthogonal matrix) and the non-zero elements are positive (i.e., does not change the phase of  $\{\mathbf{F} \mathbf{M} \mathbf{s}\}_p$ ).

The second subproblem can be expressed as

$$\begin{aligned} \mathbf{s}^{(i)} = \arg \min_{\mathbf{s}} & \frac{1}{\sqrt{N}} \|\mathbf{F}^H \mathbf{M} \mathbf{s} - \sqrt{P} \mathbf{A} \boldsymbol{\theta}^{(i)}\|_2 + \lambda \|\mathbf{s}\|_{\infty} \\ \text{s.t.} & \quad c_1: \{\mathbf{s}\}_{\frac{L-1}{2}} = 0 \\ & \quad c_2: \Re\{\{\mathbf{F}^H \mathbf{M} \mathbf{s}_i\}_0\}, \Im\{\{\mathbf{F}^H \mathbf{M} \mathbf{s}\}_0\} \leq u_{\text{first}} \\ & \quad c_3: \Re\{\{\mathbf{F}^H \mathbf{M} \mathbf{s}\}_p\}, \Im\{\{\mathbf{F}^H \mathbf{M} \mathbf{s}\}_p\} \leq u_{\text{leak}}, p \in \mathbb{N}_{\text{low}}. \end{aligned} \quad (8)$$

In (8), the quadratic constraints  $c_2$  and  $c_3$  in (6) are replaced with the linear constraints which limit the imaginer and real components of the samples instead of their powers to simplify the problem. Since (8) is a convex optimization problem, it can be solved by using solvers such as SeDuMi [17].

The cost function in (6) always decreases when (7) and (8) are solved iteratively since the global optima for both (7) and (8) can be obtained. After certain termination condition is met, the optimized sequence  $\bar{\mathbf{s}}$  is obtained as  $\bar{\mathbf{s}} = \sqrt{P} \times \mathbf{s}^{(i)} / \|\mathbf{s}^{(i)}\|_2$ .

#### IV. NUMERICAL RESULTS

In this section, we numerically evaluate the sequences generated through the method derived in Section III-B. For the evaluations, we adopt the IEEE 802.11n/ac OFDM parameters, i.e.,  $T_s = 3.2 \mu\text{s}$ ,  $\Delta f = 312.5 \text{ kHz}$ , and  $T_{\text{CP}} = 0.8 \mu\text{s}$ . We generate the basis functions in  $\mathcal{W}$  by using  $L = 15$  adjacent tones. We consider four different optimized sequences by using the parameter sets given by  $\{u_{\text{leak}} = u_{\text{first}} = 1\text{e-}3, \lambda = 0, T_{\text{active}} = 1.2 \mu\text{s}\}$ ,  $\{u_{\text{leak}} = u_{\text{first}} = 1\text{e-}3, \lambda = 2.2, T_{\text{active}} = 1.2 \mu\text{s}\}$ ,  $\{u_{\text{leak}} = u_{\text{first}} = 1\text{e-}4, \lambda = 0, T_{\text{active}} = 1.6 \mu\text{s}\}$ , and  $\{u_{\text{leak}} = u_{\text{first}} = 1\text{e-}4, \lambda = 2.2, T_{\text{active}} = 1.6 \mu\text{s}\}$ . For the optimization, the initial sequence  $\mathbf{s}^{(0)}$  is chosen as an all-ones vector of length 15. The optimized sequences for  $b_m = 0$  are listed in Table I. In the simulations,  $f_{s_1}(t)$  is generated by circularly shifting  $f_{s_0}(t)$  in time by  $T_{\text{active}}$ .

##### A. Time and Frequency Characteristics

The corresponding waveforms for the sequences in Table I are provided in Figure 1. While the first and the second sequences confine the energy on the duration of  $1.2 \mu\text{s}$ , the third and the fourth sequences keep the energy on the first half of  $T_s$ , i.e.,  $1.6 \mu\text{s}$ . Therefore, for the same amount of bit energy,

Table I: Sequences

| Sequence #1  | Sequence #2   | Sequence #3 | Sequence #4   |
|--------------|---------------|-------------|---------------|
| 0.117∠22.5°  | 0.692∠266.19° | 0.031∠180°  | 0.225∠50.42°  |
| 0.375∠315.0° | 0.986∠211.15° | 0.171∠90°   | 0.705∠324.83° |
| 0.784∠247.5° | 1.119∠157.37° | 0.509∠0°    | 1.175∠242.64° |
| 1.221∠180.0° | 1.119∠115.63° | 1.023∠270°  | 1.225∠170.47° |
| 1.480∠112.5° | 1.119∠80.70°  | 1.489∠180°  | 1.052∠122.68° |
| 1.367∠45.0°  | 1.119∠34.18°  | 1.557∠90°   | 1.225∠74.16°  |
| 0.826∠337.5° | 0.735∠337.50° | 1.011∠0°    | 0.980∠0°      |
| 0∠0°         | 0∠0°          | 0∠0°        | 0∠0°          |
| 0.826∠22.5°  | 0.735∠22.50°  | 1.011∠0°    | 0.980∠0°      |
| 1.367∠315.0° | 1.119∠304.18° | 1.557∠270°  | 1.225∠254.16° |
| 1.480∠247.5° | 1.119∠215.70° | 1.489∠180°  | 1.052∠122.68° |
| 1.221∠180.0° | 1.119∠115.63° | 1.023∠90°   | 1.225∠350.47° |
| 0.784∠112.5° | 1.119∠22.37°  | 0.509∠0°    | 1.175∠242.64° |
| 0.375∠45.0°  | 0.986∠301.15° | 0.171∠270°  | 0.705∠144.83° |
| 0.117∠337.5° | 0.692∠221.19° | 0.031∠180°  | 0.225∠50.42°  |

the first and the second sequences cause more peaky signals in time as compared to the third and the fourth sequences. On the other hand, the first and the second sequences allow smoother transitions between adjacent symbols in WUS since the CP portion of the corresponding waveforms do not contain high energy samples. This is due to the fact that there are no high-energy samples on the last  $0.8 \mu\text{s}$  of the corresponding waveforms for  $b_m = 0$  and  $b_m = 1$ . It is also worth noting that these sequences are compatible with the WURs which cannot discard the CP duration since the energy is localized either on the first or the last  $2 \mu\text{s}$ . In addition, They can be utilized for the waveforms which generate an internal guard interval within IDFT duration (e.g., [18]).

When  $T_{\text{active}}$  is reduced to  $1.6 \mu\text{s}$  to  $1.2 \mu\text{s}$ , the leakage on the OFF duration increases. As shown in Figure 1, the ratio between the peak values on the ON and OFF durations is approximately 78 dB for the third sequence whereas it reduces to 49.5 dB for the first sequence. This reduction is due to the fact that  $\mathbb{M}_{\text{low},i}$  becomes a larger set while  $L$  is fixed. When  $\lambda$  is 0, there is no penalty applied for the non-uniform power distribution of the sequence elements. When  $\lambda$  is set to 2.2 to control the power distribution, the difference between the maximum levels on the ON and OFF durations reduces further to 23.2 dB and 45 dB for the second and the fourth sequences, respectively. The power distribution over the subcarriers for each sequence are given in Figure 2. The first and the third sequences allocate more energy on 6-8 tones while the second and the fourth sequences have more uniform power distribution across the 15 tones at the expense of more leakage in time.

##### B. BER Performance for Standalone Scenarios

In Figure 3, we evaluate the BER performance when the proposed sequences and the other available OOK waveform options, i.e., turning on and off the carrier (single tone) and mask-based approach proposed in [9], are utilized. For multipath channel, we assume that  $\mathcal{L} = 10$  and  $\tau = 0.1$  at the sample rate of 20 MHz. We set the sample rate of the WUR to 20 MHz. Note that the sample rate of the WUR can be decreased to reduce the power consumption of the WUR. In this case, the corresponding BER curve for WUR in Figure 3 needs to be shifted to the right proportionally. We assume that the cut-off frequency  $f_c$  of LPF at WUR is

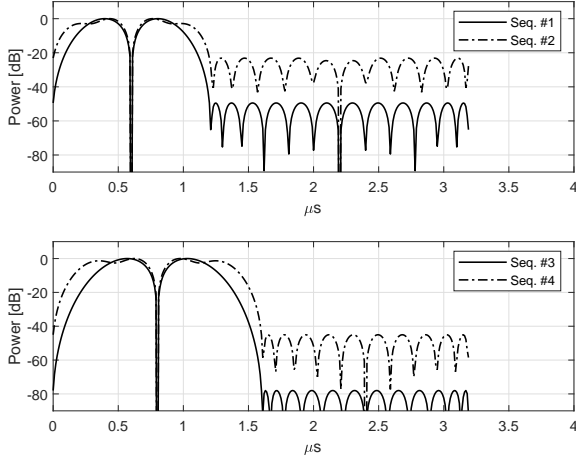


Figure 1: The transmitted waveform when  $b_m = 0$ , i.e.,  $f_{s_0}(t)$ .

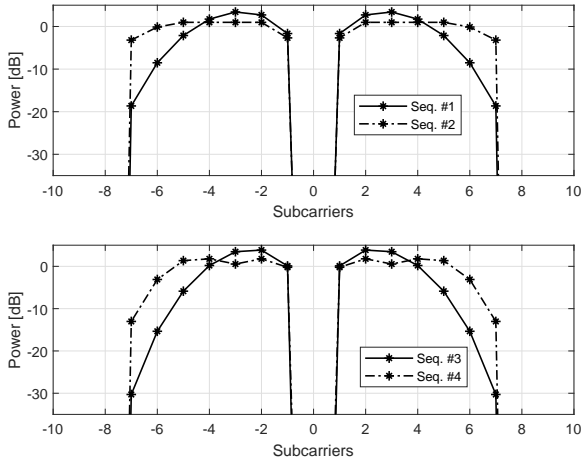


Figure 2: Power distribution of the sequences over the subcarriers.

2.5 MHz. As shown in Figure 3, all of the OOK waveforms are at least 6 dB worse than the BER performance of the QPSK symbols in the additive white Gaussian noise (AWGN) channel. This is due to the fact that the Euclidean distance between the bits is  $1/\sqrt{2}$  times that of the QPSK symbols and the non-coherent detection is used at the WUR. In AWGN, the BER performances for different OOK options are similar to each other. The sequence options which cause shorter  $T_{\text{active}}$  duration perform slightly better as compared to the ones with larger  $T_{\text{active}}$  duration. This improvement is because the WUR accumulates less noise energy when  $T_{\text{active}}$  is small. The second sequence is slightly worse than the first sequence due to its higher leakage on the OFF duration. Nevertheless, because of less noise accumulation, the second sequence perform better than the third and the fourth sequences although it has a higher leakage at the OFF period. In AWGN, single tone, mask-based method, the third sequence, and the fourth sequences performs almost identical. However, in fading channel, the performance of single tone dramatically deteriorates as it does

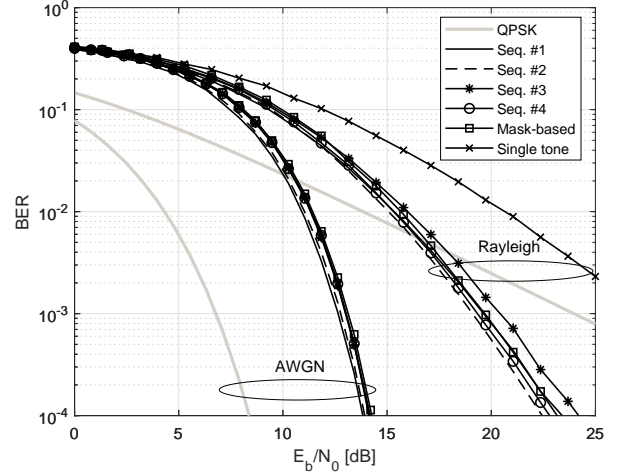


Figure 3: Standalone BER performance.

not exploit the frequency selectivity. The other options are within the margin of 1.5 dB. The best performance is achieved by the second sequence since the power is well-distributed in frequency as compared to others and a shorter  $T_{\text{active}}$  is adopted. The third sequence is the worst one as the energy of the sequence is localized in frequency as shown in Figure 2 and large  $T_{\text{active}}$  causes more noise accumulation.

### C. BER Performance under Multiplexing

In Figure 4, we evaluate the BER performance of the OFDM and WUR receivers when WUS and QAM symbols are multiplexed in frequency. We assume that WUS is scheduled to the center of the band, i.e.,  $\{-7, \dots, 7\}$  tones. The QAM symbols are allocated to the adjacent subcarriers where the tone indices are  $\{-16, \dots, -10, 10, \dots, 16\}$ . We assume that signal power for WUS and OFDM symbol are identical and half of the signal power is distributed to 14 QAM symbols. The signal-to-noise ratio (SNR) is calculated at 20 MHz sample rate. We evaluate two waveform options for WUS, i.e., the proposed scheme with the second sequence and the mask-based method proposed in [9]. In Figure 4a, the BER performance at the WUR is provided. The LPF is able to filter out the QAM symbols on adjacent tones and the BER performance at WUR for both approaches acceptable. The order of the BER curves follows the same order in Figure 3. On the other hand, the OFDM receiver is sensitive to the existence of WUS. As shown in Figure 4b, the BER performance at the OFDM receiver degrades drastically when mask-based OOK is utilized for WUS. The degradation is because the mask-based OOK symbols are not orthogonal to the OFDM symbol and contaminate the adjacent tones which are utilized by QAM symbols. On the other hands, the WUS with the proposed scheme is always orthogonal to the subcarriers used for QAM symbols and do not degrade the performance at the OFDM receiver since the WUS waveform is generated within the OFDM framework.

## REFERENCES

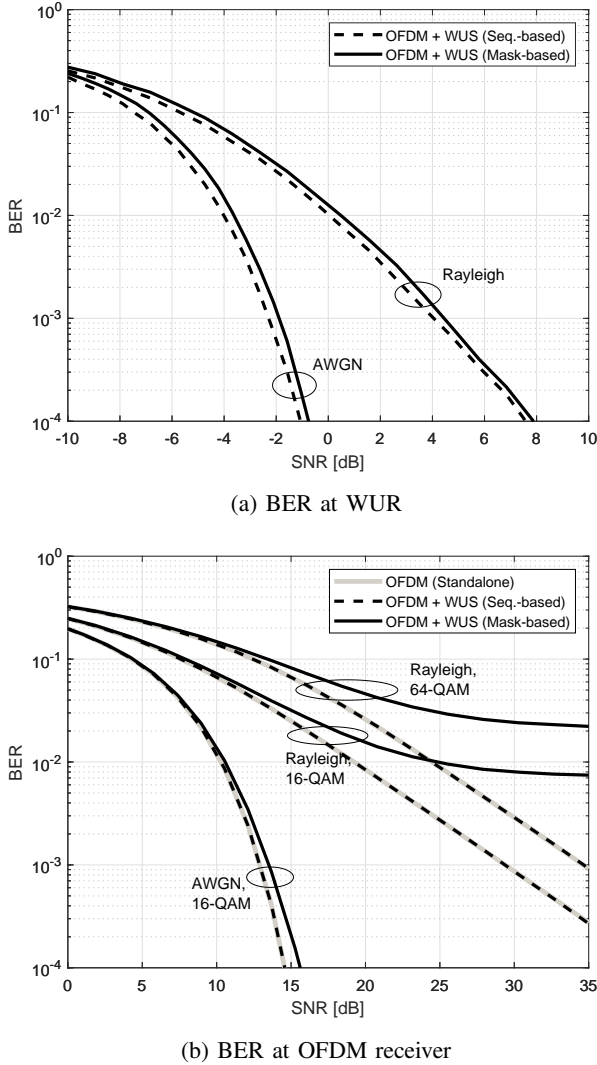


Figure 4: BER performance when WUS and QAM symbols are multiplexed in frequency

## V. CONCLUDING REMARKS

In this study, we propose a method which generates OOK symbols by using sequences in the frequency domain. The proposed method does not cause any interference to the adjacent subcarriers and enables orthogonal multiplexing of WUSs and OFDM waveforms. We derive the sequences with a tractable algorithm relying on CAN and demonstrate the performance of four optimized sequences by considering the leakage on the OFF period and the flatness of the corresponding waveforms in time and frequency. The numerical results show that the proposed approach removes the interference-floor at OFDM receiver when OFDM-based waveforms and WUS are multiplexed in the frequency domain. In addition, the WUR performance is improved when the energy distribution of a coded OOK symbol in frequency is even and the leakage on the OFF period is low. Multiplexing multiple WUSs, obtaining scalable expressions of the sequences, and packing more than two OOK symbols within one OFDM symbol duration are several directions for the extension of this work.

- [1] H. S. Kim and D. D. Wentzloff, "Back-channel wireless communication embedded in wfi-compliant ofdm packets," *IEEE Journal on Selected Areas in Communications*, vol. 34, no. 12, pp. 3181–3194, Dec 2016.
- [2] J. Im, H. S. Kim, and D. D. Wentzloff, "A 335  $\mu$ w -72dbm receiver for fsk back-channel embedded in 5.8ghz Wi-Fi ofdm packets," in *2017 IEEE Radio Frequency Integrated Circuits Symposium (RFIC)*, June 2017, pp. 176–179.
- [3] S. Tang, H. Yomo, and Y. Takeuchi, "Optimization of frame length modulation-based wake-up control for green w lans," *IEEE Transactions on Vehicular Technology*, vol. 64, no. 2, pp. 768–780, Feb 2015.
- [4] N. E. Roberts, K. Craig, A. Shrivastava, S. N. Wooters, Y. Shakhsher, B. H. Calhoun, and D. D. Wentzloff, "26.8 a 236nw ???56.5dbm-sensitivity bluetooth low-energy wakeup receiver with energy harvesting in 65nm cmos," in *2016 IEEE International Solid-State Circuits Conference (ISSCC)*, Jan 2016, pp. 450–451.
- [5] H. Zhang, C. Li, S. Chen, X. Tan, N. Yan, and H. Min, "A low-power ofdm-based wake-up mechanism for ioe applications," *IEEE Transactions on Circuits and Systems II: Express Briefs*, vol. 65, no. 2, pp. 181–185, Feb 2018.
- [6] R. Piyare, A. L. Murphy, C. Kiraly, P. Tosato, and D. Brunelli, "Ultra low power wake-up radios: A hardware and networking survey," *IEEE Communications Surveys Tutorials*, vol. 19, no. 4, pp. 2117–2157, Fourthquarter 2017.
- [7] "PAR: Part 11: Wireless lan medium access control (mac) and physical layer (phy) specifications amendment: Wake-up radio operation," P802.11ba, Sep. 2016.
- [8] D. K. McCormick, "IEEE technology report on wake-up radio: An application, market, and technology impact analysis of low-power/low-latency 802.11 wireless lan interfaces," *802.11ba Battery Life Improvement: IEEE Technology Report on Wake-Up Radio*, pp. 1–56, Nov 2017.
- [9] V. Kristem, S. Azizi, and T. Kenney, "2 us OOK waveform generation," IEEE 802.11-18/0492r2, 2018.
- [10] A. Sahin, R. Yang, X. Wang, H. Lou, and F. L. Sita, "On the coexistence of 802.11ax and 802.11ba signals," IEEE 802.11-18/0659r1, May 2017.
- [11] P. Stoica, H. He, and J. Li, "New algorithms for designing unimodular sequences with good correlation properties," *IEEE Transactions on Signal Processing*, vol. 57, no. 4, pp. 1415–1425, Apr. 2009.
- [12] —, "On designing sequences with impulse-like periodic correlation," *IEEE Signal Processing Letters*, vol. 16, no. 8, pp. 703–706, Aug 2009.
- [13] H. He, P. Stoica, and J. Li, "Designing unimodular sequence sets with good correlations - including an application to MIMO radar," *IEEE Transactions on Signal Processing*, vol. 57, no. 11, pp. 4391–4405, Nov. 2009.
- [14] M. Soltanalian, M. M. Naghsh, and P. Stoica, "A fast algorithm for designing complementary sets of sequences," *Signal Processing*, vol. 93, no. 7, pp. 2096 – 2102, 2013. [Online]. Available: <http://www.sciencedirect.com/science/article/pii/S0165168413000613>
- [15] T. Erdélyi, "Polynomials with Littlewood-type coefficient constraints," *Michigan Math. J.*, vol. 49, pp. 97–111, 2001.
- [16] P. Erdős, "Some unsolved problems." *Michigan Math. J.*, vol. 4, no. 3, pp. 291–300, 1957.
- [17] J. Sturm, "Using SeDuMi 1.02, a MATLAB toolbox for optimization over symmetric cones," *Optimization Methods and Software*, vol. 11–12, pp. 625–653, 1999, version 1.05 available from <http://fewcal.kub.nl/sturm>.
- [18] G. Berardinelli, F. M. L. Tavares, T. B. Sørensen, P. Mogensen, and K. Pajukoski, "Zero-tail DFT-spread-OFDM signals," in *IEEE GLOBE-COM Workshops (GC Wkshps)*, Dec 2013, pp. 229–234.